DOI: https://doi.org/10.52651/sam.j.2022.2

SCIENCE & MILITARY

No 2 | Volume 17 | 2022

SCIENCE & MILITARY

The rationale for publishing this periodical by the Armed Forces Academy of General Milan Rastislav Štefánik is to enable the authors to publish their articles focused on particular scientific issues in the following areas: Military science, Natural Sciences, Engineering and Technology.

Original scientific articles will be published twice a year.

Published by: Armed Forces Academy of General Milan Rastislav Štefánik, Demänová 393, 031 01 Liptovský Mikuláš, Slovak Republic. IČO 37 910 337. Registered No: EV 2061/08. ISSN 1336-8885 (print). ISSN 2453-7632 (online).
DOI: http://doi.org/10.52651/sam.j.2022.2

Printed by: Armed Forces Academy of General Milan Rastislav Štefánik, Demänová 393, 031 01 Liptovský Mikuláš, Slovak Republic. Order forms should be returned to the editorial office. Published biannually.
The subscription rate for one year is 7,30 €.
The journal Science & Military is included in following multiple databases: EBSCO. ProQuest Central: PQ Science Journals; PQ Military Collection; PQ Computing; PQ Telecommunications; Illustrata: Technology; Forthcoming Technology Research Database (TRD) full text packages.

Address of the editorial office
SCIENCE & MILITARY
Armed Forces Academy of General Milan Rastislav Štefánik, Demänová 393, 031 01 Liptovský Mikuláš,
Slovak Republic
Phone: +421-960-423065 Fax: +421- 044-55 222 47 E-mail: redakcia@aos.sk http://sm.aos.sk

DOI: https://doi.org/10.52651/sam.j.2022.2

SCIENCE & MILITARY

No 2 | Volume 17 | 2022

Dear readers,

Science and society can advance thanks to effective scientific communication, which is a fast growing phenomenon owing to the global network called the Internet. Publishing has become an inseparable part of scientific work. It plays an essential role in promoting research and it has a positive influence not only on authors' profiles but also on reputation of colleges and universities they work for. Nowadays, research results are mostly published in scientific journals. Prestigious journals, especially those which are listed in databases such as SCOPUS, WOS, etc., have enormous information potential. The editorial board of the Science & Military journal has made a considerable number of steps so that the journal meets the selection criteria and can be indexed in the SCOPUS database. The Science & Military journal has already been added to open access publishing platforms that support the Budapest Open Access Initiative (BOAI), the main purpose of which is to make research articles under the Creative Commons license freely available to as many readers as possible. Our journal, however, can move forward only thanks to high-quality scientific papers that will map the moving boundaries of human knowledge and will properly contribute to debates among academics in Slovakia as well as abroad.

Dear readers and authors, the future of the Science & Military journal depends especially on your articles and readers' positive responses. That is why I would like to offer all researchers and teachers at universities as well as doctoral students an opportunity to publish the results of their scientific work in the Science & Military.

Dear readers, let me briefly introduce the papers that the latest issue of the journal contains. I believe that they will inspire you and that they will initiate scientific discussions.

The first among the peer-reviewed articles in this issue is the article titled ***"Suitability of Using Different Types of Shotgun Shells in Defence Against Low-Slow-Small UAVs"*** *written by Ivan Pemčák, Jiří Skala and Josef Bača. This paper examines the suitability of using different types of shotgun shells for defence against low, slow and small (LSS) UAVs (Unmanned Aerial Vehicles). It also presents the theoretical procedure for determining the optimal types of shotgun ammunition depending on the distance and resistance of the target.*

The following article written by Miroslav Pacek and Zdeněk Matoušek titled ***"Analysis of Relevant Energetic Proportions for Elint Activities in the HF Frequency Band"*** *deals with an algorithm for analysis of some relevant energetic proportions of skywave propagation, with consideration of Electronic Intelligence in the high-frequency band. In terms of Electronic Intelligence, Radio-Electronic object is represented by the Over-The-Horizon radar.*

Among the articles in this issue, you can find the paper written by Viktor Dolinaj and Miroslav Marko titled ***"Tribotechnical Diagnostics – Engine Oil (MO) Characteristics Control Mogul Diesel DR SAE 20W50 T-72"****. The article presents a very interesting and current topic of malware detection and provides an initial insight into the complex subject of antivirus protection. In this article, the internal components of AV programs and well-known packing techniques are briefly explained while, in addition, they are tested against each other.*

The series of articles is closed with the paper titled ***„Measurement of the Resolution of the Mounted Periscope of the Armoured Vehicle"*** *written by Jozef Bača, Ivan Pemčák and Kateřina Nováčková. The aim of this paper is to clarify the way of measuring the image intensifier device with variable extinction ratio of an incoming illumination. It is possible to simulate the threshold conditions of the device usage in field conditions.*

Dear readers, on my behalf and on the behalf of the editorial board, I would like to wish you all the best in the upcoming year and thank you for your readers' interest.

Brig. Gen. (ret.) Assoc. Prof. Eng. Boris ĎURKECH, CSc.
Chairman of the Editorial Board

Reviewers

Lt. Dipl. Eng. Martin **BARTOŠ**, PhD.	Armed Forces Academy of General M. R. Štefánik, Lipt. Mikuláš, SK
LtCol. Dipl. Eng. Marek **HOVANEC**, PhD.	General Staff of the Armed Forces of the Slovak Republic, SK
LtCol. Dipl. Eng. Jozef **DUDÁŠ**, PhD.	General Staff of the Armed Forces of the Slovak Republic, SK
Assoc. Prof. Dipl. Eng. Vladimír **POPARDOVSKÝ**, PhD.	Armed Forces Academy of General M. R. Štefánik, Lipt. Mikuláš, SK
Assoc. Prof. Dipl. Eng. Marie **RICHTEROVÁ**, PhD.	University of Defence Brno, CZ

DOI: https://doi.org/10.52651/sam.a.2022.2.5-10

SUITABILITY OF USING DIFFERENT TYPES OF SHOTGUN SHELLS IN DEFENCE AGAINST LOW-SLOW-SMALL UAV

Ivan PEMČÁK, Jiří SKALA, Josef BAČA

Abstract: The suitability of using different types of shotgun shells for defence against low, slow and small (LSS) UAVs (Unmanned Aerial Vehicle) is investigated in this article. The basic criterion for assessing the effectiveness of shotgun fire is the hit probability and the effect of gunfire on the target. When using different types of shotgun ammunition, it is necessary to balance two conflicting requirements. First is hit probability which is affected by the number of pellets in the shotgun shell. Second is the kinetic energy of pellets which is affected by their size and speed. The theoretical procedure for determining the optimal types of shotgun ammunition depending on the distance and resistance of the target is demonstrated.

Keywords: Hit probability; Kinetic energy of pellet; UAV; Buckshot; Birdshot; Shotgun dispersion.

1 INTRODUCTION

Today, the use of unmanned aerial vehicles (UAVs) is widespread in both civilian and military applications. Increasing the availability of these devices to the general public also means an increased security risk. For companies, in terms of industrial espionage, and for the armed and security forces, in terms of reconnaissance and direct attack. In this article will be discussed defence against micro UAV of Class I. [1] Properties of this subclass of UAVs are described in Table 1.

Tab. 1 Properties of Micro Class I. UAVs

Weight of UAV	Operating Altitude	Mission Radius	Payload
< 2.00 kg	< 90 m	< 5 km	0.2-0.5 kg

Source: author.

Defence against UAVs is currently composed form many different methods. These methods range from control signal jamming, GPS scrambling, taking control of the device, to the physical capture or destruction of the device. Signal jamming may become less and less effective in the future, due to the implementation of autonomous systems that do not rely on GPS signal or operators input. Therefore, it is necessary to have the means for physical destruction of UAVs. One way of physical destruction is the use of small arms fire. And one of the most common groups of handheld weapons for defensive purposes is the shotgun. The effective range of most shotgun shells is limited by the relatively low initial velocity and high dispersion of the pellets cloud. At the same time, shotgun ammo offers large variability between individual types of rounds, differing in the number of shots, their size, material and initial speed.

This article was created in collaboration with the Department of Weapons and Ammunition, University of defence Brno. This article is one of a series dealing with the detection and elimination of UAVs. [2][3]

2 DETERMINATION OF BASICS PARAMETERS

Two types of cartridges were chosen for comparison in this article. In American terminology, these are the 12 gauge #4 Buckshot and the #1 Birdshot. Equivalent designation of used ammunition is 12/76/6,09mm SB and 12/70/4,00mm SB. Cartridges are displayed in Fig. 1. Properties of the cartridges used are described below in Table 2.

Fig. 1 #1Birdshot (left) and #4 Buckshot (right) shels
Source: author.

Tab. 2 Ammunition properties

Type	Number of pellets	Pellet diameter (mm)	Weight of one pellet (g)	Initial velocity (m/s)
#4 Buckshot	41	6,09	1,32	370
#1 Birdshot	111	4	0,323	380

Source: author.

The number of pellets and their weight was determined by delaboration of used ammunition. The initial speed of the cluster of shots was provided by the manufacturer of ammunition. [4][5] In both cases, the pellet was made from lead. The cartridges were chosen with regard to their availability and its use in the Czech army.

3 DETERMINING THE PROBABILITY OF TARGET DESTRUCTION

The basic precondition for destroying the target is its hit with sufficient number of projectiles with sufficient energy. It is not certain, that pellet form shot will hit the target. Therefore, it is necessary to first determine the hit probability. Simulation method will be used to determine the hit probability. In this paper, is considered as the target of a commercially available drone DJI MAV 2. Whose 3D model is used for creation of image of drone in a target plane Fig. 2. For this paper was chosen random orientation of drone. In this image, drone is divided into two areas.

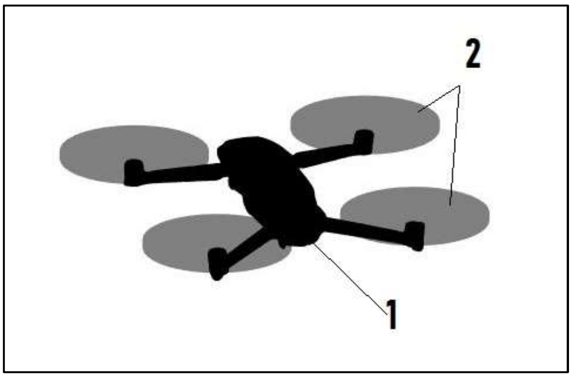

Fig. 2 Used drone image - DJI MAV 2
Source: author.

The first area consists of the drone body itself,. I assume that a single shot of any size with kinetic energy greater than $E_{k,\,lim}$ will ensure destruction. The second area consists of rotor spaces. Which is the entire space where the rotor moves. It would be impractical to simulate firing with individual rotors in different positions, so this simplification is introduced. As a result, the rotor is not necessarily hit when rotor space is hit. To facilitate the calculation, I assume that the probability of the rotor blade being hit in case of hit rotor space is P_{rot} = 0.2. This problematic will be detailly investigated in future studies. For purposes of this article, this simplification is acceptable. Also in this case, the kinetic energy necessary to eliminate the propeller and thus the entire drone is considered to be $E_{k,lim}$. Combined hit probability for entire drone $P_{1,2}$ is calculated as

$$P_{1,2} = P_1 + P_2 P_{rot}. \qquad (1)$$

Where P_1 and P_2 are probabilities for hitting each part of drone.

3.1 Determining the probability of hit

To determine the probability of hitting the target when firing a cloud of projectiles, it is necessary to determine the characteristics of the dispersion of the cluster of shots depending on the distance, this dependence is known as „pattern". To do this, experimental shootings were carried out. For this experiment was used Beneli M3T with 19.75 inches smoothbore barrel with cylinder bore (without choke). Targets were analysed using Matlab code. [6]

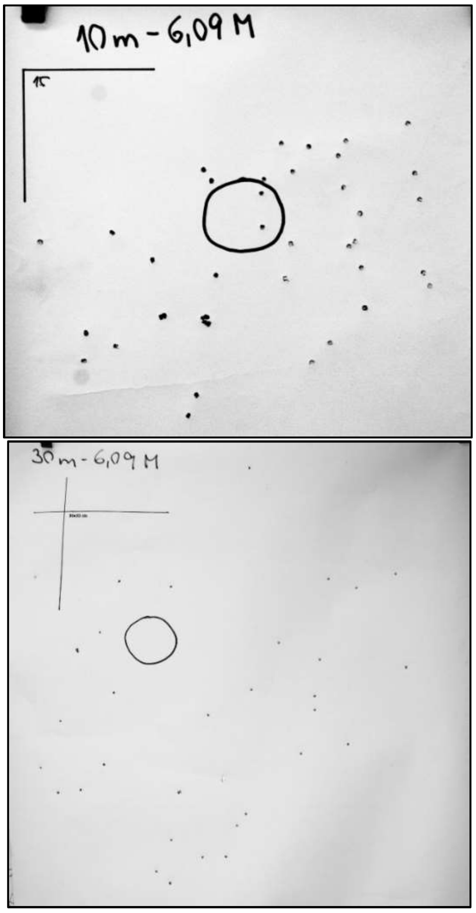

Fig. 3 Pattern for #4 Buckshot at 10m (top) amd 30m (bottom)
Source: author.

In Fig. 3 are shown targets after one shot of #4 Buckshot at distances 10m and 30m with circle with 10cm in diameter used as aiming point. Note that in both cases, the midpoint of impact is shifted to the right and bottom. This shift was also observed in other targets. It is result of imperfect zeroing of the weapon. It is a systematic mistake removable by correctly zeroing of the weapon.

In this article, I will not take into account the error of the shooter or the error of aiming the weapon. The aiming error also includes an error of determining distance and lead. This issue is described in previous articles in this series [1] [2].

Distribution of hits corresponded to the normal distribution. This was confirmed by analysis carried out in Matlab using Shapiro-Wilk parametric hypothesis test of composite normality with α = 0.05. [3] Furthermore, it can be assumed that when shooting shotgun horizontally at short distances, σx, σy will be the same. Thus, the scattering pattern should have a circular characteristic. Minor deviations from this assumption observed in Table 2 are possibly caused by an insufficient number of conducted experiments. The following characteristics were determined and used for calculations.

Tab. 3 Standart deviation of shots from center of pattern

Standard deviation from the centre of pattern in mm (σ_x, σ_y)			
Type	10m	20m	30m
#4 Buckshot	120, 89	213, 213	235, 263
#1 Birdshot	77, 85	176, 161	244, 332

Source: author.

For further calculations were standard deviation approximated by first degree polynomial equations. Values of 0 for both σ_x and σ_y were added at 0m distance for proper approximations. Equations for dispersion with 95 % confidence bounds are shown below.

$$\sigma_{x,\#4\ Buck} = (7.98 * x + 22), \quad (2)$$

$$\sigma_{y,\#4\ Buck} = (9.13 * x + 4), \quad (3)$$

$$\sigma_{y,\#1\ Bird} = (8.31 * x), \quad (4)$$

$$\sigma_{y,\#1\ Brid} = (10.72 * x - 16{,}4). \quad (5)$$

Results for #4Buckshot were further verified by another experiment. In which was fired at square target of size 0,6m x 0,6m at distance 10m – 50m in 10m increments. Two independent targets were used. Number of hits in each target was counted. Hit counts were compared with simulation of fire at target 0,6m x 0,6m using Monte Carlo method with 10000 individual experiments for each distance. Results of simulation are compared in Tab. 4. Shot at Target 1. at 50m distance was admitted as shooters error.

Tab. 4 Hit count ouf #4 Buckshot

	Distance to target (m)				
	10	20	30	40	50
Target 1	41	36	21	11	3
Target 2	41	38	14	12	9
Simulation	41	33	22	15	10

Source: author.

Due to the insufficient number of experiments for proper statistical evaluation, I consider these results to be satisfactory for this article. With the obtained dispersion parameters, it was possible to simulate, the probability of hit for individual target zones for both types of shells. The centre of dispersion pattern was aimed at the centre mass of drone.

In Fig. 4 are shown results of one simulation for #4 Buckshot in distance 10 and 30 meters. Each red point represents one pellet hit in target plane.

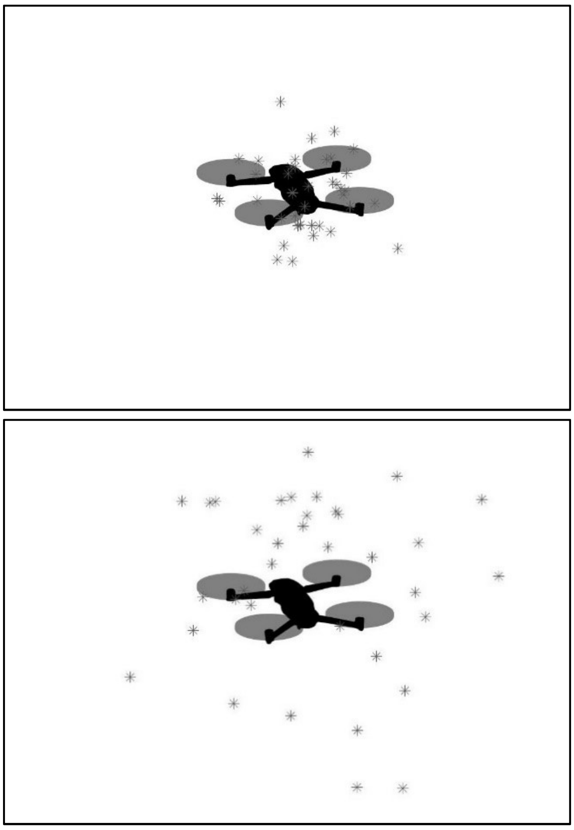

Fig. 4 Dispersion simulation in 10 (top) and 30 meters (bottom)
Source: author.

Simulations were carried out using Monte Carlo method with 10000 individual experiments for a given distance with a step of 5m. In each experiment was examined the state of target. If at least one pellet hit was observed in first zone, the target was considered to be destroyed. When pellet hit second zone, then was tested dependent probability of hitting rotor blade.

If rotor blade was hit, then the target was destroyed. With large number of experiments the frequency of successful destruction of the target is equal to the probability of destruction.

The results of the simulations are shown in Fig. 5.

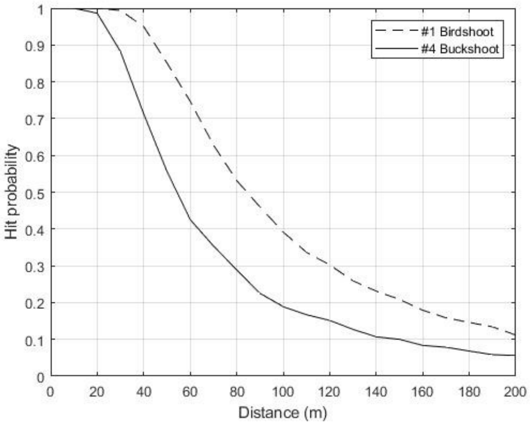

Fig. 5 Combined hit probability for both types of ammunition
Source: author.

It is clear from the results, that the use of #1 Birdshot is more advantageous in terms of hit probability. For example, at 50 m has the #1 Birdshot probability $P_{\#1\ \mathrm{Bird},\ 50} = 0.84$ when for #4 Buckshot it is only $P_{\#4\ \mathrm{Buck},\ 50} = 0.45$. However, the energy of the projectile must be taken into account when assessing effectiveness of fire.

3.2 Determination of projectile energy

For the needs of this paper, the energy of individual projectiles was considered to be equal its kinetic energy

$$E_k = \frac{1}{2} m v^2. \tag{6}$$

Where m is mass of single pellet and v is instantaneous speed of projectile. The calculation of the speed of projectile fired from firearms is one of the basic tasks of external ballistics and is described in detail in the literature [7] [8]. Since the shotgun pellets are spherical, it was possible in this article to use the simplified calculation method presented by E.J. Allen in publication "Approximate ballistics formulas for spherical pellets in free flight" [9]. Equation 6. Calculate speed of single pellet at given distance and is divided into three parts depending on Mach's number of projectile.

$$v = \begin{cases} \dfrac{0{,}92 M_0 v_S}{(0{,}92 + 0{,}0375 M_0) e^{\left(\frac{0{,}69x}{k_Z}\right)} - 0{,}0375 M_0} & for\ 0 < x \le x_1 \\ \dfrac{-0{,}1956 v_S}{0{,}965 e^{\left(\frac{-0.12225(x - x_1)}{k_Z}\right)} - 1{,}128} & for\ x_1 < x \le x_2 \\ \dfrac{0.2926 v_S}{0{,}495 e^{\left(\frac{0{,}3135(x - x_2)}{k_Z}\right)} - 0{,}077} & for\ x > x_2 \end{cases} \tag{7}$$

where:

$$x_1 = 1{,}44928\, k_z \cdot \ln\left(\frac{0.80417 M_0}{0.92 + 0.0375 M_0}\right), \tag{7}$$

$$x_2 = x_1 + 1{,}05173 k_z\ , \tag{8}$$

$$k_z = \frac{D \rho_p}{\rho_a}, \tag{9}$$

$$M_0 = \frac{v_0}{v_s}, \tag{10}$$

where v_0 is initial velocity of projectile, v_s speed of sound, D is diameter of projectile, ρ_p is density of projectile material, ρ_a is density of air and x is distance from muzzle. For this paper values were chosen as:

$$\rho_\mathrm{p} = 11{,}3\ \mathrm{g \cdot cm^{-3}},$$

$$\rho_a = 0{,}0012\ \mathrm{g \cdot cm^{-3}},$$

$$v_s = 340\ \mathrm{m \cdot s^{-1}}.$$

The dependence of speed on the flight path was determined by analytical calculation. The calculated speeds correlate with the observation and are shown in Fig 6.

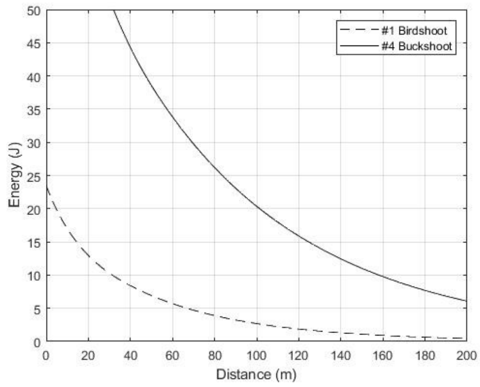

Fig. 6 Kinetic energy of individual pellets for both types of ammunition
Source: author.

Required kinetic energy needed for drone destruction is considered to be $E_{\mathrm{k,lim}} = 10\mathrm{J}$. The value was chosen on the basis of practical experience. It can be seen from the speed profiles that #1 Birdshot has kinetic energy only 6.9 J at 50 m, which is less than the estimated limit energy $E_{\mathrm{k,lim}} = 10\mathrm{J}$. In contrast, #4 Buckshot with 38J of energy is certainly capable to destroy intended target.

4 DESIGN OF THE OPTIMAL SHOTGUN LOAD FOR A GIVEN DISTANCE

The calculated results show that the # 4 Buckshot is too powerful for its intended purpose because its kinetic energy does not correlate with the probability of a hit. With the obtained outputs, it is possible to theoretically design the optimal load with the maximum probability of hit and sufficient energy at the selected distance of the engagement. To demonstrate this case, we choose a distance of 100m.

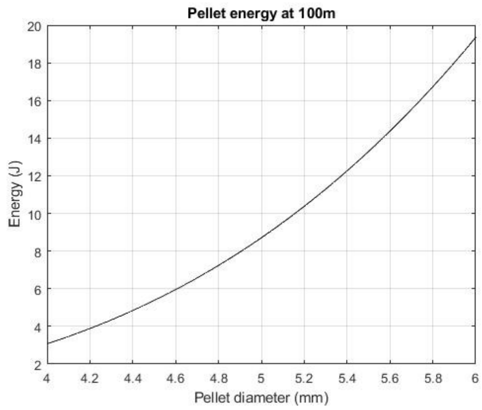

Fig. 7 Pellet energy at 100m
Source: author.

Using formula from the previous paragraph, it is possible to numerically quantify the kinetic energy of a pellet at a distance of 100 m with initial speed $v_0 = 370\ \mathrm{m \cdot s^{-1}}$, depending on its the diameter. This v_0 is the most common among powerful heavy high-brass loads. Iteration step is selected as 0.01mm. The resulting energies are shown in Fig. 7.

When energy E_k = 10J is required at a distance of 100 m, a pellet with a diameter should be D = 5,15mm. This shotgun load is closely related to the not very widespread ammunition marked as AAA Buckshot. This load is currently difficult to obtain and is usually manufactured only for chambers of length of 70mm and shorter, while the described # 4 Buckshot is designed for more powerful systems with a chamber length of 76mm. Therefore, some data from the # 4 Buckshot are used for the theoretical load calculation. For purpose of this paper this theoretical load will be called AAA Buckshot 12/76. It is expected that the total weight of the shots will be the same, as are used for optimal load calculation. The total weight of pellets in the cartridge is given by the relation

$$m_s = c_p * m_p. \tag{11}$$

Where m_s is the weight of all pellets in cartridge, c_p is the number of pellets in the cartridge and m_p is weight of one pellet. Substituting the data from Tab. 1 for #4 Buckshot we get $m_{s,\#4}$ = 54,12g. By expressing and substituting the equation is obtained:

$$c_{p,AAA.12/76} = \frac{m_{s,\#4}}{m_{p,AAA}}, \tag{12}$$

Where $$m_{p,AAA} = \frac{\pi * D^3}{6} * \rho_p, \tag{13}$$

It can be assumed that the initial speed of the pellet cloud will be the same for #4 Buckshot and designed AAA Buckshot 12/76.

Tab. 5 Properties of eperimental load

Type	Number of pellets	Pellet diameter (mm)	Weight of one pellet (g)	Initial velocity (m/s)
AAA Buckshot 12/76	66	5,15	0.808	370

Source: author.

By reducing the diameter of an individual pellet and maintaining the total weight of all pellets in the cartridge, the cartridge will naturally contain a larger number of pellets. This will consequently also increase probability of successful hit. For calculation was used dispersion properties of # 4 Buckshot. Based on experience, this simplification can be used for preliminary analysis. For exact verification scatter pattern, it is necessary to perform experimental shooting, which is outside the scope of this article.

The simulation results using the values for AAA Buckshot 12/76 are shown in the following graph.

It can be observed that the limit energy of 10J is reached at a distance of 100m. At this distance there is a probability of hit $P_{\text{AAA Buck 12/76, 100}}$ = 0.37. For comparison $P_{\text{\#4 Buck, 100}}$ = 0.20.

5 CONCLUSION

This article presents possible way of evaluating effectiveness of shotgun fire. It can be stated that at the specified parameters, the use of #1 Birdshot ammunition is ineffective for distances exceeding 30m. Birdshot ammunition in general can only be used effectively for a very short distance. At the same time, it can be stated that the use of ammunition #4 Buckshot at a distance of 50 m still guarantees the probability of hitting $P_{\text{\#4 Buck, 50}}$ = 0.5 with more than enough energy for the effect in the target.

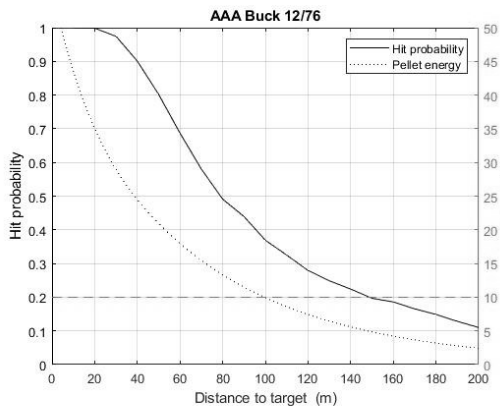

Fig. 8 Energy of pellet and hit probability of theoretical AAA Buckshot 12/76
Source: author.

Furthermore, the procedure for determining the optimal load for a given distance of 100 m was demonstrated. In which sufficient energy $E_{k,lim} = 10J$ is still provided for destruction of chosen target. If desired maximal distance would be lower, even smaller diameter pellet could be used resulting in higher hit probability. Simultaneously with increasing resistance of the targets and required kinetic energy of pellet, the question arises of using larger shots, for example popular #00 Buckshot, even at the cost of a lower hit probability. Which then have to be adequately balanced by a larger number of shooters, or several rounds fired at given target.

In this article the dispersion characteristics of the Benelli M3T shotgun and used ammunition used were significantly simplified, for exact application it is necessary to exactly confirm their specification and experimentally verify the presented results.

References

[1] BIRCH, G. C., J. C. GRIFFIN and M. K. ERDMAN. *UAS Detection, Classification, and Neutralization: Market Survey.* Market Survey prepared by Sandia National Laboratories, Sandia Report SAND 2015-6365, 2015. Available at: https://doi.org/10.2172/1222445

[2] RACEK, F., T. BALÁŽ, J. KREJČÍ, M. MACKO and S. PROCHÁZKA.Tracking, aiming and hitting the UAV with ordinary assault rifle. In *Counterterrorism, Crime Fighting, Forensics, and Surveillance Technologies.* Bellingham, WA 98227-0010 USA: SPIE-INT SOC OPTICAL ENGINEERING, 2017, p. "104410C-1"-"104410C-11". ISSN 0277-786X. ISBN 978-1-5106-1346-1.

[3] KREJČÍ, J., T. BALÁŽ and M. ŠVEC. Methods for determining of UAS hit probability In *Conference Proceedings of ICMT'21*. Brno: University of Defence, 2021. Vol. 2021. Available at: https://doi.org/10.1109/ICMT52455.2021.9502765

[4] Ammunition manufacturer's. Available at: https://www.sellier-bellot.cz/produkty/brokove-naboje/lovecke-naboje-magnum-a-buck-shot/detail/30/

[5] Matlab support. Available at: https://www.mathworks.com/matlabcentral/fileexchange/13964-shapiro-wilk-and-shapiro-francia-normality-tests

[6] BAKYTOVA, H. *Basics of statistics.* 2nd edition. Bratislava: Alfa, 1979.

[7] JIRSÁK, Č. and P. KODYM. *Vnější balistika a teorie střelby 2.* Praha: Naše vojsko, 2017. ISBN 978-80-206-650-0.

[8] ALLEN, E. J. Approximate ballistics formulas for spherical pellets in free flight. In *Defence Technology*. Volume 14, Issue 1. MSC: 76N15 34C60. Available at: https://doi.org/10.1016/j.dt.2017.11.004

[9] Image Processing Toolbox™User's Guide. © COPYRIGHT 1993–2021 by The MathWorks, Inc.

Dipl. Eng. Ivan **PEMČÁK**
University of Defence
Kounicova 65
662 10 Brno
Czech Republic
E-mail: ivan.pemcak@unob.cz

Dipl. Eng. Jiří **SKALA**
University of Defence
Kounicova 65
662 10 Brno
Czech Republic
E-mail: jiri.skala@unob.cz

Dipl. Eng. Josef **BAČA**
University of Defence
Kounicova 65
662 10 Brno
Czech Republic
E-mail: josef.baca@unob.cz

Ivan PEMČÁK graduated in Weapons and ammunition engineering from University of Defense, Czech Republic in 2018. After two-year as an ordnance officer in a light infantry battalion of Czech armed forces, he returned to the University of Defense as Ph.D. candidate. His field of research is fire control systems, target hit probability and weapon design.

Jiří SKALA graduated in Weapons and ammunition engineering from University of Defense, Czech Republic in 2020. He is currently employed at Prototypa-ZM, s.r.o. as an experimental shooter and technician. In parallel with work, he is working on his PhD at the Department of Weapons and Ammunition His field of research is weapon design, operation and maintenance.

Josef BAČA graduated in Weapons and ammunition engineering from University of Defense, Czech Republic in 2017. He serves in the military repair facility in Jaroměř, where he specializes in the repair of fire control systems. His field of research is fire control systems, target acquisition and optical system design.

DOI: https://doi.org/10.52651/sam.a.2022.2.11-17

ANALYSIS OF RELEVANT ENERGETIC PROPORTIONS FOR ELINT ACTIVITIES IN THE HF FREQUENCY BAND

Miroslav PACEK, Zdeněk MATOUŠEK

Abstract: Intelligence as a warfighting function is a continuous process. It is carried out before planning the mission, during the preparation of the mission, and during its execution as well. The results of the intelligence warfighting function enable commanders to predict the course of action for potential threats and facilitate the commander´s decision-making process. If intelligence information is derived from foreign communication (Communication Intelligence) and noncommunication (Electronic Intelligence) electromagnetic radiations by other than intended recipients, we are speaking about Signals Intelligence. Communication and noncommunication foreign emitters might be also denoted as Radio-Electronic objects. This paper presents an algorithm for analysis of some relevant energetic proportions of a skywave propagation, with consideration of Electronic Intelligence in the high-frequency band. In terms of Electronic Intelligence, Radio-Electronic object is represented by the Over-The-Horizon radar.

Keywords: Electronic intelligence; Radio-electronic object; Over-the-horizon radar; Energetic proportions; High-frequency band.

1 INTRODUCTION

Over-the-horizon (OTH) radars operate in the high frequency (HF) band (3÷30 MHz). They are using the reflection of electromagnetic (EM) energy from the ionosphere (ionized layer of the atmosphere) for their operation. Detection and tracking of airborne, maritime, and ground targets by OTH radars is usually done by a far larger distance than by radars operating on the Line-Of-Sight principle. That fact also represents the main advantage of OTH radars- to execute surveillance over a distance exceeding thousands of kilometers from its own territory [1],[2].

The main application of OTH radars is within ballistic missile early warning systems for long-range detection. Such a system is composed of varied technical means, which detect the launch of an intercontinental ballistic missile (ICBM), estimate its probable trajectory, and provide given information to the higher level of command or to the predefined entities (military units or decision makers). That kind of early warning system has usually two main components, a ground-based component (OTH radars), and a space component (space-based surveillance) [3].

All components of the ballistic missile early warning system are usually on high alert and are working in continuous operation in order to provide information about possible adversary´s ICBM. Essential information for early warning systems is mainly gathered during tests of newly developed ICBM or during regular periodic tests of ICBM already deployed within strategic rocket forces [3].

2 ELECTRONIC INTELLIGENCE

When conducting Electronic Intelligence (ELINT) activities, gathered intelligence is derived from intercepting noncommunication signals. The value of ELINT is that it provides timely information about threatening systems, such as radars that guide aircraft or missiles to targets [4].

For successful fulfillment of given tasks, it is necessary to configure ELINT receivers in space and time in a way, that enables proper interception of Radio-Electronic objects (REO). Configuration of REO on the one hand and ELINT receivers on the other hand, both in space and time, together with some necessary preconditions for processing radio signals might be called the ELINT chain. An example of the ELINT chain for the OTH radar operating in the HF frequency band is shown in Figure 1.

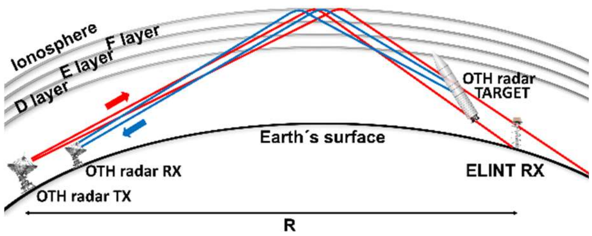

Fig. 1 An example of the ELINT chain for the OTH radar operating in the HF frequency band
Source: author.

The proposed example of the ELINT chain illustrates the basic principle of the EM energy propagation between the transmitter (TX) antenna of OTH radar (representing REO in this specific scenario) and the antenna of the ELINT system (intercepting OTH radars).

2.1 Basic aspects for properly functioning ELINT chain

The basic attributes for a properly functioning ELINT chain are as follows:

1. Securing mutual directivity of antenna arrays, for both REO antenna and ELINT system antenna.
2. Securing frequency tuning of ELINT receiver to the carrier frequency of the REO signal.
3. Having sufficient power level of transmitted EM energy by OTH radar, so the power level of a signal on the ELINT receiver input $P_{inELINT}$ is sufficient for further processing. This precondition is denoted by

$$P_{inELINT} \geq P_{P\min} , \tag{1}$$

while the sensitivity of the ELINT receiver P_{Pmin} is expressed as [4]

$$P_{P\min} = k \cdot T_0 \cdot F \cdot B \cdot \frac{S}{N} , \tag{2}$$

where k is the Boltzmann constant, T_0 is the absolute temperature, F is a noise factor, B is a signal bandwidth and S/N is the required ratio between signal to noise at the receiver input.
4. Securing the same mode of operation (modulation) for both- REO and ELINT system.
5. Securing identical polarization of EM energy for both- REO and ELINT system.

Basic energetic parameters for a properly functioning ELINT chain are as follows:
1. $P_{inELINT}$ is the power level of a signal on the ELINT receiver input.
2. P_{TX} is the power level of a signal on the REO TX output.
3. G_{TX} is the antenna gain of REO TX.
4. $G_{inELINT}$ is the antenna gain of an ELINT receiver.
5. R is the distance between the REO TX antenna and the ELINT receiver antenna.

3 SKYWAVE PROPAGATION

The ionosphere is a part of Earth's upper atmosphere with a high concentration of electrons to such a degree, that it can affect the propagation of EM energy. It is a result of the ionization process caused mainly by solar activity. According to the current ionization degree, it may vary from 60 ÷ 600 km above the Earth's surface, while at approximately the height of 600 km it fluently transitions to the magnetosphere (600÷2000 km). Under specific conditions, the ionosphere can reflect EM energy with an exactly defined carrier frequency. [5],[6]

Up to the height of 100 km, the composition of the atmosphere is constant; while 78% is represented by N_2, 21% is represented by O_2, and the rest is represented by other gases. At higher altitudes, molecules of oxygen and nitrogen are dissociated by solar activity to the atoms accordingly by [7]

$$\begin{aligned} O_2 + h\omega &\rightarrow O + O \ , \\ N_2 + h\omega &\rightarrow N + N \ , \end{aligned} \tag{3}$$

where $h\omega$ is a quantum of incident energy, ω is the angular frequency of the radiation and h is the Planck constant.

4 ANALYSIS OF ENERGETIC PROPORTIONS FOR HF FREQUENCY BAND

There are two propagation modes for the HF frequency band, groundwave propagation, and skywave propagation. Skywave propagation is used for transmissions over long distances when EM waves are reflected from various layers of the ionosphere. The carrier frequency of an EM wave determines from which ionosphere layer will be EM wave reflected. When considering skywave propagation, it is also necessary to take into account variations of the ionosphere based on time and space (geographical) conditions.

The highest carrier frequency when the reflection from the ionosphere is still taking place is called critical frequency f_{CR} denoted by [7]

$$f_{CR} = \sqrt{80.8 \cdot N_{\max}} \ , \tag{4}$$

where N_{max} is the maximum electron density.

The critical frequency is one of the basic parameters, which determines the condition of the ionosphere. For every layer within the ionosphere, there is a critical frequency. Critical frequencies usually vary in a range of 1 ÷ 16 MHz. EM energy with a carrier frequency higher than the critical frequency would not reflect from the ionosphere but will penetrate the upper layers of the atmosphere.

For a successful mode of operation in the HF frequency band, maximum usable frequency is defined as [8]

$$MUF = \frac{f_{CR}}{\cos(\varphi)} = f_{CR} \cdot \sec(\varphi) \ , \tag{5}$$

where φ is the oblique incidence angle striking the ionosphere.

The electric field strength E at the distance R from the REO (at the ELINT receiver) for one-hop skywave propagation is denoted by [9]

$$\begin{aligned} E_{[dB]} = {} & 136.6 + 20\log(f)_{[MHz]} + 10\log(P_{TX})_{[kW]} + \\ & + G_{TX[dB]} - L_{is[dB]} \ , \end{aligned} \tag{6}$$

where the f is a carrier frequency, P_{TX} is a power level on the TX output, G_{TX} is a TX antenna gain and L_{is} is the loss of the EM energy for a skywave propagation.

Loss of the EM energy for a skywave propagation $L_{is[dB]}$ is denoted by [9]

$$L_{is[dB]} = L_{0[dB]} + L_{a[dB]} + L_{M_{[dB]}} + L_{g_{[dB]}} + L_{h[dB]} + L_{z[dB]} \ , \tag{7}$$

where L_0 is the free-space path loss, L_a is the ionosphere absorption loss, L_m is the above MUF loss, L_g is summed ground-reflection loss at intermediate reflection points, L_h is auroral and other signal losses in terms of the geomagnetic latitude and L_z is another non-specified loss (current recommended value is 9.9 dB).

4.1 Free-space path loss

In terms of Free-space EM energy propagation, Free-space path loss (spreading loss) is expressed as [10]

$$L_0 = \left(\frac{4 \cdot \pi \cdot R}{\lambda} \right)^2, \tag{8}$$

where R is the transmission distance and λ is the wavelength of the carrier signal.

The formula for spreading loss determined in dB is characterized as [9]

$$L_{0[dB]} = 20 \cdot \log\left(\frac{4 \cdot \pi \cdot R}{\lambda} \right), \tag{9}$$

or by the so-called Friis transmission formula [10]

$$L_{0[dB]} = 32.45 + 20\log(f)_{[MHz]} + 20\log(R)_{[km]}, \tag{10}$$

where f is the frequency of the carrier signal and R is the transmission distance.

The transmission distance R, which also represents the effective length of the transmission link is in the case of skywave propagation defined as the trajectory of EM energy over the distance D (oblique path distance) by the formula [9]

$$D = 2 \cdot n \cdot \sqrt{\left(\frac{R}{2} \right)^2 + h^2}, \tag{11}$$

where n is the number of reflections from the ionosphere, R is the ground distance between TX (OTH radar) and RX (ELINT receiver), and h is the height of the ionosphere layer used for reflection.

Adding equation (11) into equation (10) yields

$$L_{0[dB]} = 32{,}45 + 20\log f_{[MHz]} + \\ +20\log\left[2 \cdot n \cdot \sqrt{\left(\frac{R}{2} \right)^2 + h^2} \right]. \tag{12}$$

The elevation angle is determined by [7]

$$tg(\alpha) = \left[\cos(\psi) - \frac{R_Z}{R_Z + h} \right] \cdot \sin(\psi) = \frac{2h}{R} - \frac{R}{4R_Z}, \tag{13}$$

where h is the reflection height of the ionosphere and ψ is the half of an angle within a circular segment illustrating the ground distance between TX and RX and R_Z is the Earth radius.

Angle ψ is defined by an equation [7]

$$\psi = \frac{R}{222.4}. \tag{14}$$

The incidence angle striking the ionosphere is expressed as [7]

$$\varphi = \arctan\left\{ \frac{R_Z \cdot \sin(\psi)}{h + R_Z \cdot [1 - \cos(\psi)]} \right\}. \tag{15}$$

A basic principle of skywave propagation is shown in Figure 2.

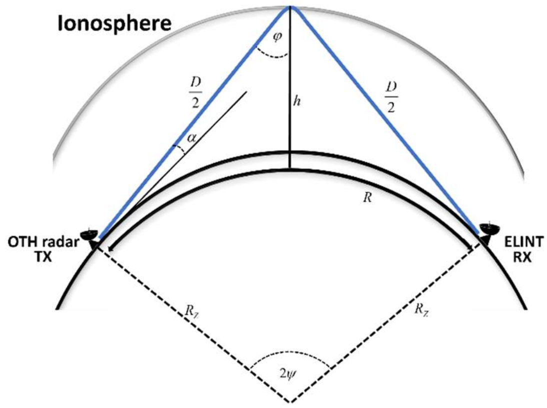

Fig. 2 A basic principle of skywave propagation
Source: author.

In the case of planning skywave propagation for very long distances (for over 10 000km – which is not the case for OTH), it is necessary to consider also so-called focusing gain G_f denoted as [9]

$$G_f = 20 \cdot \log\left(\left| 1 - \frac{n \cdot \pi \cdot R_Z}{R} \right| \right), \tag{16}$$

where n is the number of reflections from the ionosphere, R_Z is the Earth radius, R is the transmission distance and π is the ratio of a circle's circumference to its diameter.

In that specific case, equation (10) will be modified to [9]

$$L_{0[\mathrm{dB}]} = \left[32.45 + 20\log_{10}(f)_{[\mathrm{MHz}]} + 20\log_{10}(D)_{[\mathrm{km}]} \right] - \\ -G_{f[\mathrm{dB}]}, \tag{17}$$

where f is the frequency of the carrier signal, D is the oblique path distance and G_f is the focusing gain.

4.2 Skywave propagation loss

The skywave propagation loss is mostly dependent on the directional properties of an antenna, elevation angle, and incidence angle. Overall loss of skywave propagation L_{is} has multiple components, such as free-space path loss, ionosphere absorption loss, above *MUF* loss, summed ground-reflection loss, auroral and other signal losses in terms of the geomagnetic latitude, and other non-specified losses.

4.2.1 Ionosphere absorption loss

The highest absorption of EM energy in the ionosphere occurs in the D layer at a height of approximately 50÷90 km. Electron density in this layer is two to three times lower than in the E and F layers. That level of ionization is not sufficient for the effective reflection of EM energy in the HF frequency band. If the direction of EM energy propagation is not affected, we are speaking about non-deviative absorbing. The highest absorption in the D layer is present during summer at noon. [11]

On the other hand, deviative absorbing significantly changes the direction of EM energy. That is typical for the E layer of the ionosphere. In practice, overall absorption at the D and E layers is approximately 1 dB. As mentioned before, absorption is mostly dependent on electron density, which differs day and night. Daytime absorption for the D and E layers is expressed as [9]

$$L_a = n.\frac{6.667 \cdot \sec(i)}{(f + f_L)^{1,98} + 10.2} \cdot I \ , \qquad (18)$$

where f_L is the gyrofrequency in the E layer at 100 km, i is the incidence angle at 100km and I is the absorption coefficient.

The absorption coefficient is denoted as [9]

$$I = (1 + 0.0037R_{12}) \cdot \left[\cos(0.881\chi)\right]^{1/3} \ , \qquad (19)$$

where R_{12} is a 12-month smoothed sunspot number and χ is a solar zenith angle.

The incidence angle at 100km i is calculated by [9]

$$i = \arcsin\left[0.985 \cdot \cos(\varphi)\right] \ . \qquad (20)$$

Night-time absorption for the D and E layers is expressed as [9]

$$L_a = \frac{(7 + 0.019 \cdot D) \cdot (1 + 0.015 \cdot R_{12})}{f^2 + 10} \ . \qquad (21)$$

4.2.2 The above MUF loss

Using a higher carrier frequency than *MUF* results in a considerable loss L_M. If the carrier frequency is equal to or lower than *MUF*, then $L_M=0$. In other cases, the above *MUF* loss L_M is expressed as [9]

$$L_M = 130 \cdot \left[\frac{f}{MUF} - 1\right]^2 \ . \qquad (22)$$

4.2.3 Summed ground-reflection loss

For more than one hop skywave propagation, summed ground-reflection loss L_g must be taken into account. Ground-reflection loss L_g is denoted by [9]

$$L_g = 2 \cdot (n - 1) \ , \qquad (23)$$

where n is a hop number.

4.2.4 Auroral and other signal losses

Auroral loss L_h depends on geomagnetic latitude G_n and local time. If geomagnetic latitude meets criterion $G_n \leq 42.5°$, then auroral loss L_h=0. In other cases, auroral loss L_h is determined by an empiric table [9].

4.2.5 Non-specified losses

Non-specified losses L_Z are defined as other types of losses, which may occur during EM energy propagation. The recommended value for L_Z during planning the HF propagation path is 9.9 dB [9].

4.3 Power level on the receiver input

For communication links using skywave propagation up to 7000 km, the power level on the receiver input $P_{inELINT}$ is [9]

$$P_{inELINT[\mathrm{dBW}]} = E_{[\mathrm{dB}]} + G_{RX[\mathrm{dB}]} - 20\log(f)_{[\mathrm{MHz}]} - 107.2 \ , \quad (24)$$

where E is the electric field strength in distance R from the REO (transmitting antenna) calculated by (6) and G_{RX} is an ELINT receiver antenna gain.

The given formula does not comprise eventual losses caused by the line transmission losses, neither for the transmitter nor for the receiver.

A defined mathematical model describes energetic proportions. It also gives assistance to the theoretical evaluation of skywave propagation in order to conduct electronic intelligence. An illustration of energetic proportions in the ELINT chain for the OTH radar is shown in Figure 3.

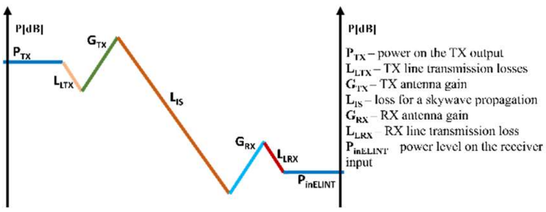

Fig. 3 Illustration of energetic proportions in the ELINT chain for the OTH radar
Source: author.

5 ALGORITHM FOR ANALYSIS OF RELEVANT ENERGETIC PROPORTIONS OF A SKYWAVE PROPAGATION

Energetic proportions of the skywave propagation were described in previous chapters. In practical applications, those calculations might be done in one sequence. In that case, the proposed algorithm might be used. Having such an algorithm enables the prediction of propagation losses, thus yielding awareness about energetic proportions for the ELINT chain. The proposed algorithm for analysis of some relevant energetic proportions of a skywave propagation is shown in Figure 4.

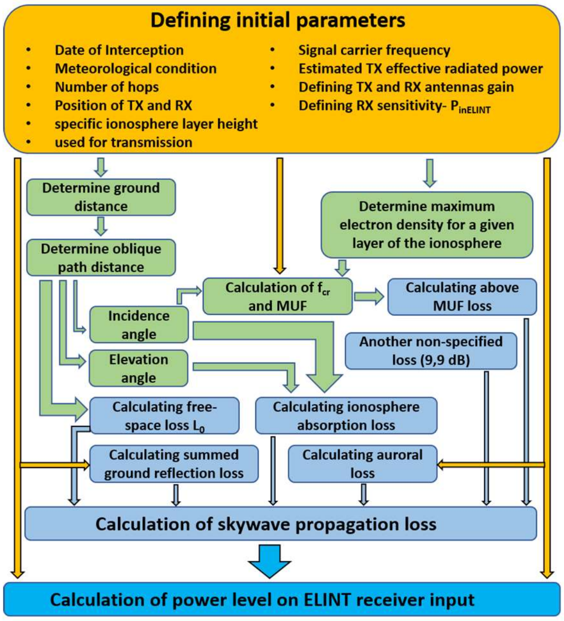

Fig. 4 Algorithm for analysis of some relevant energetic proportions of a skywave propagation
Source: author.

The proposed algorithm consists of four stages. During the 1st stage, the definition of initial parameters is taking place. Because the status of the ionosphere varies not only during the day but also during the seasons, a specific date for the model must be determined. Meteorological conditions might be also determined, but for the illustration of the algorithm, we will not take them into account. Based on the specific measures executed by meteorological institutions, we can define the current height of the ionosphere layer for the specific geographical location (including maximum electron density). The rest of the initial inputs are more of a technical consideration, such as the signal carrier frequency of the TX, estimated TX effective radiated power, assumed TX and RX antenna gain, and sensitivity of the ELINT receiver.

After the initial parameters are defined, the 2nd stage of the proposed algorithm is taking place. During that stage, it is necessary to calculate the ground distance between RX and TX. Based on the height of the specific layer within the ionosphere, elevation and incidence angles are calculated. Based on the given values, the calculation of an oblique distance of a skywave is determined. Calculation of f_{CR} and *MUF* might be executed according to the current status of the maximum electron density or be provided by the meteorological institution.

During the 3rd stage of the proposed algorithm, the calculation of losses and their additional summation is taking place. For the calculation of summed ground reflection loss, it is necessary to know how many hops will be used, and for the auroral loss, geomagnetic latitude is derived from the point, where the reflection from the ionosphere is assumed. All the losses are calculated by the equations shown in Chapter 4.

The final stage of the proposed algorithm is calculating the power level on the ELINT receiver input. Based on the calculated power level on the ELINT receiver input, we can determine if the interception of the REO is feasible.

The proposed algorithm was designed in the MATLAB computing platform.

6 THE ALGORITHM VERIFICATION FOR ANALYSIS OF RELEVANT ENERGETIC PROPORTIONS OF A SKYWAVE PROPAGATION

The results of the proposed algorithm were verified by the VOACAP software. VOACAP software is free software used for the prediction of HF communications links. For verification purposes, the initial parameters for both, the proposed algorithm and VOACAP, were as follows:

1. Date of interception was 291200ZJUL22.
2. No extreme meteorological conditions.
3. No failure is expected on the RX and TX.
4. One hop of a skywave is considered.
5. REO is not using a higher frequency than *MUF*.
6. F2 layer for reflection will be used.
7. The height of an F2 layer is 245 km.
8. MUF for the F2 layer on a given day is 16 MHz.
9. $G_{TX[dB]}=0$ and $G_{RX[dB]}=0$.

Based on the input data, the skywave propagation loss by the proposed algorithm was determined as $L_{is} = 131.325\ dB$. The power level of a signal on the ELINT receiver input was determined as $P_{inELINT} = -88.916\ dBW$. However, in some cases, signal on the receiver input is not specified in the power level, but in the voltage for the specific impedance *Z*. The given value expressed in dBW might be converted to the voltage value for an impedance of 50 Ω by the formula [12]

$$U_{[\mathrm{dB\mu V}]} = P_{[\mathrm{dBW}]} + 137 . \quad (23)$$

Hence $P_{inELINT} = -88.916\ dBW$ is after conversion equal to $U_{inELINT} = 48.16\ dB\mu V$.

The skywave propagation loss by VOACAP was determined as $L_{is} = 132.5\ dB$. An example of the skywave propagation loss executed by VOACAP software is shown in Figure 5.

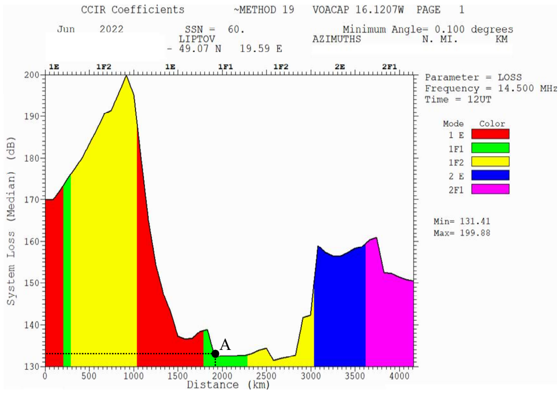

Fig. 5 An example of the skywave propagation loss executed by VOACAP software
Source: author.

The level of a signal on the ELINT receiver input by VOACAP was determined as $U_{inELINT} = 44\ dB\mu V$. An example of the level of a signal on the ELINT receiver input by VOACAP software is shown in Figure 6.

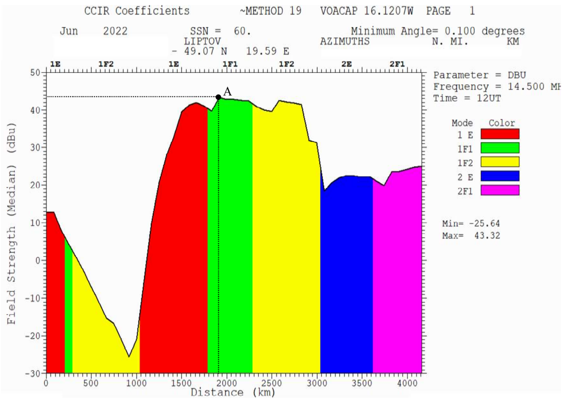

Fig. 6 An example of the level of a signal on the ELINT receiver input by VOACAP software
Source: author.

In the case of loss calculations, the proposed algorithm deviated by 1.175 dB, which is a good performance. When values of the signal level on the ELINT receiver input are compared, the difference is 4.16 dBμV, which is still acceptable. In that case, a higher difference might be caused by additional consideration of complementary effects during the skywave propagation in the VOACAP software.

7 CONCLUSION

Detection and subsequent location of OTH radars is becoming an actual issue. OTH radars as REO are providing crucial information for ELINT and subsequently for air defense and anti-ballistic missile systems, hence representing a source for the decision-making process on the strategic level of command.

When conducting ELINT activities, having awareness of energetic proportions is an inevitable precondition for a successfully executed operation.

Based on the abovementioned analysis for a specific case study, we can conclude that monitoring of OTH is possible for distances over thousands of km. OTH radars are generally bistatic systems and their transmitting power is usually somewhere around tenths of kW. When using radio frequency direction finding for OTH location, it is possible to use not only amplitude based but also phase based methods.

The proposed algorithm designed in the MATLAB computing platform provides evaluations of energetic proportions for the ELINT chain, thus enabling successfully executed ELINT operations.

References

[1] FABRIZIO, G. *High Frequency Over-the-Horizon Radar.* New York: McGrawHill, 2013. ISBN 978-0-07-162140-3.

[2] KOLOSOV, A. A. *Over the Horizon Radar.* Boston: Artech house, 1987. ISBN 0-89006-233-1.

[3] PODVIG, P. L. *Istoria i sovremennoe sostoane rossijskoj sistemy preduprezhdenia o raketnom napadenii, centr po izucheniu problem razoruzhenia, energetiki i ekologii.* Moscow: Moskovskij fiziko-technicheskij institut, 2002.

[4] WILEY, R. G. *ELINT - The Interception and Analysis of Radar Signals.* Boston: Artech House, 2006. ISBN 1-58053-925-4.

[5] DAVIES, K. *Ionospheric Radio Propagation.* Washington: US Department of Commerce, 1965. Available at: https://doi.org/10.6028/NBS.MONO.80

[6] CAROZZI, T. D. *Radio Waves in the Ionosphere: Propagation, Generation and Detection*. Uppsala: Swedish Institute of Space Physics, 2000. ISSN 0284-1703.

[7] HÁCHA, B. *Šíření rádiových vln.* Časť II. 1. vyd. Liptovský Mikuláš: VVTŠ, 1990.

[8] PROKOP, J. a J. VOKURKA. *Šíření elektormagnetických vln a antény.* Praha: SNTL/ALFA, 1980.

[9] ITU-R Radiocommunication Sector of ITU: Method for the prediction of the performance of HF circuits, ITU-R P.533-14, 2019.

[10] MATOUŠEK, Z., J. OCHODNICKÝ a A. HYKEL. *Šírenie elektromagnetickej energie a vodičové antény.* 1. vyd. Liptovský Mikuláš: Akadémia ozbrojených síl generála M. R. Štefánika v Liptovskom Mikuláši, 2006. ISBN 80-8040-306-6.

[11] PECHAČ, P. a S. ZVÁNOVEC. *Základy šíření vln pro plánování pozemních rádiových spojů.*

1. vyd. Praha: BEN – technická literatura, 2007. ISBN 978-80-7300-223-7.
[12] ADAMY, D. *EW101: A first course in electronic warfare.* Boston: Artech House, 2001. ISBN 1-58053-169-5.

Dipl. Eng. Miroslav **PACEK**
Armed Forces Academy of General M. R. Štefánik
Department of Electronics
Demänová 393
031 01 Liptovský Mikuláš
Slovak Republic
E-mail: miroslav.pacek@aos.sk

Assoc. Prof. Dipl. Eng. Zdeněk **MATOUŠEK**, PhD.
Armed Forces Academy of General M. R. Štefánik
Department of Electronics
Demänová 393
031 01 Liptovský Mikuláš
Slovak Republic
E-mail: zdenek.matousek@aos.sk

Miroslav PACEK – was born in Humenné, Slovakia in 1986. He received his M.Sc. (Eng.) at the Armed Forces Academy of general Milan Rastislav Štefánik in Liptovský Mikuláš. He started his dissertation studies in 2021 and his research is focused on ELINT. Currently, he is working as a fellow at the Department of Electronics, Armed Forces Academy of general Milan Rastislav Štefánik in Liptovský Mikuláš.

Zdeněk MATOUŠEK – was born in Frýdlant, Czech Republic in 1961. He received a M.Sc. (Eng.) from the Radar Technology Department, Military Academy in Liptovský Mikuláš in 1985. In 2000 he successfully finished his PhD. studies in electrical engineering. In 2008 he finished his habilitation thesis at the University of Defence in Brno, Czech Republic. Currently, he is working as an associate professor at the Electronics Department, Armed Forces Academy of general Milan Rastislav Štefánik in Liptovský Mikuláš. His areas of research are intelligence, electronic intelligence, RF antennas and radio electronics systems.

DOI: https://doi.org/10.52651/sam.a.2022.2.18-25

TRIBOTECHNICAL DIAGNOSTICS - ENGINE OIL (MO) CHARACTERISTICS CONTROL MOGUL DIESEL DT SAE 20W50 T-72

Viktor DOLINAJ, Miroslav MARKO

Abstract: This work is performed by tribotechnical diagnostics, specifically by checking the properties of motor oil type Mogul Diesel DT SAE 20W-50 used in heavy combat equipment, such as the T-72M1 tank. The work consists of expressing basic knowledge about measuring devices, which were used in the measurements and their properties and their operation. The work also contains basic knowledge about the measured liquid, which is a necessary aspect for the possibility of performing measurements. The practical part of this work consists of measurements and more detailed specification of oil properties and monitoring of its gradual degradation with the help of individual measuring instruments. All measurements were performed in the diagnostics laboratory of the Department of Mechanical Engineering at the Armed Forces Academy of General Milan Rastislav Štefánik (hereinafter„AFA") in Liptovský Mikuláš.

Keywords: Engine oil; ACEA; API; SAE; Analysis; Properties; Viscosity; Kinematics; T-72M1; Sample; Measuring instrument.

1 INTRODUCTION

The measurement of engine oil properties was performed on engine oil from a vehicle that belongs to the series of the Armed Forces of the Slovak Republic, the vehicle is a Tank T-72M. The measurements were performed at the Department of Mechanical Engineering in the AFA Tribodiagnostics Laboratory, where we used three different measuring instruments to measure the properties. A device known as FerroCheck 2000 was used to measure the Ferroparticle content, SpectroVisc-Q3050 on the kinematic properties and FluidScan Q1000 was used to measure the oil content properties.

The measurements performed were carried out in accordance with the rules and safety principles, which are short work at these facilities. After the measurement, we evaluated the results and compared them with the parameters of the reference sample.

Fig. 1 Laboratory of tribodiagnostics, AFA
Source: authors.

Fig. 2 Tribodiagnostic Laboratory - SpectroVisc Q3050-blue, Spectro Q1000 Fluidscan-yellow
Source: authors.

2 MEANS OF MEASUREMENT MO-MOGUL SAE 20W50 IN THE LABORATORY OF TRIBODIAGNOSTICS AFA AND THE MEASURED BUILDING T-72

The measurements were performed in the laboratory of tribodiagnostics in the AFA, the laboratory of tribodiagnostics is equipped with various means suitable for performing various measurements to determine the properties of motor oils.

The instruments used include the SpectroVisc Q3050, Spectro Q1000 Fluidscan, Spectrocube, Ferrograph, ferrocheck and many other instruments and equipment for performing scientific activities within AFA and the surrounding area.

Fig. 3 T-72M1
Source: authors.

Fig. 4 SpectroVisc Q3050, FerroCHeck 200 and Spectro Q1000 (right)
Source: authors.

3 ENGINE OIL MOGUL SAE 20W50

Mogul Diesel DT 20W-50 is a year-round engine oil of very high performance. It is made from high-quality, low-evaporation petroleum base oils obtained by modern hydrogenation technology and state-of-the-art refining additives such as oxidation and corrosion inhibitors or detergent dispersants. As already mentioned, this oil is intended mainly for year-round lubrication of highly strained diesel engines, whether trucks, buses, or heavy vehicles of the Armed Forces, such as T-72 tanks. This oil is also used in cases where a fuel with a higher sulphur content is used, as it effectively suppresses the formation of wear, corrosion and high-temperature deposits. It allows strict emission limits to be met and guarantees very long exchange periods.

Reducing scale formation and maximizing engine response.

Advantages of MO MOGUL SAE 20W50:

- ensures perfect lubrication of modern, highly loaded engines,
- is a guarantee of trouble-free year-round operation,
- ensures good start ability at low temperatures,
- prevents the formation of high-temperature deposits and low-temperature turbidity and keeps the engine clean,
- has excellent antioxidant properties guaranteeing long life of the oil,
- perfectly protects the internal parts of the engine against corrosion,
- extends the oil change period,
- is a guarantee of compliance with strict emission limits.

Performance characteristics of Mogul SAE 20W50 oil:

- ACEA E2,
- MB 228.1,
- MAN 271,
- VOLVO VDS.

Fig. 5 MO Mogul Diesel DT SAE 20W-50
Source: authors.

Characteristic Parameters:

Tab. 1 Parameters of Mogul Diesel DT SAE 20W-50 oil

Parameter	Unit	Value
Kinematic viscosity at 100 ° C	[cSt]	18,5
Kinematic viscosity at 40 ° C	[cSt]	164
Viscosity index	-	130
Flash point ° C	[°C]	238
Melting point ° C	[°C]	-24
TBN	[Mg KOH/g]	9,4

Source: authors.

3.1 Storage of Mogul Diesel DT SAE 20W-50

Store in tightly closed containers in places protected from rain, dust, high temperatures and other weather conditions. The maximum storage temperature is 40 ° C. Protect against water ingress and ensure that markings on storage containers are not removed. Do not store the product above 60 ° C, do not expose it to direct sunlight and frost.

Oil sampling from tank T-72M1

Fig. 6 Tank T-72 M1
Source: authors.

Fig. 7 Oil sampling from MAF cleaner
Source: authors.

Fig. 8 Method of oil sampling
Source: authors.

3.2 Requirements for serviceability and evaluation of engine oil parameters

- Appearance (comparison of clarity, gloss, odor and turbidity.
- Determine whether it satisfies according to its own methodology (practical and professional experience). Do not allow turbidity - matt surface with light reflection.
- Kinematic viscosity (primary and basic property for the usability of engine oil in the vehicle engine)
- Engine oil may only be operated within a viscosity range of ± 20% of the reference sample and diesel engine manufacturer's data
- Viscosity index - dependence of oil fluidity on temperature. The degree of viscosity index determines the guarantee of sufficient lubrication under operating conditions.

4 ANALYZER FERROCHECK 2000

FerroCheck 2000 is a portable benchtop analyser designed to help reduce costly vehicle and equipment failures by monitoring iron particles in all lubricating oils.

The core of FerroCheck is a pair of precise rounded coils that generate magnetic fields when powered. When a small amount of oil is introduced into one of the coils, ferroparticles such as iron, nickel and cobalt interact with the magnetic field, thus changing the current in the coils.

The magnitude of the current change is proportional to the amount of ferroparticles calibrated by weight in ppm per oil and lubricant.

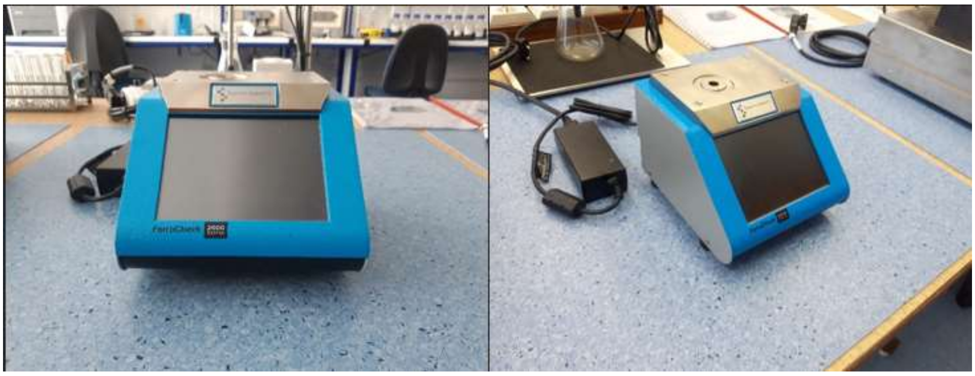

Fig. 9 FerroCheck 2000 measuring device
Source: authors.

Fig. 10 Discharge pipette for sampling
Source: authors.

4.1 Using of FerroCheck 2000

Before using the FerroCheck 2000 analyser, it is necessary to prepare a sample of the used oil, which will then be subjected to the measurement itself. In the first step, we must make sure that the particles are not at the bottom of the container from which the sample will be taken, this will be ensured by its precise mixing in a circular motion. Once we have made sure that the metal particles do not settle to thebottom of the container, we can proceed to thesubsequent sample preparation. Remove the mixed oil from the container and then fill the tube with it along the filling line, then close the tube and mix the slightly again.

Fig. 11 Oil sample tube
Source: authors.

After these operations, the measurement itself can begin, after starting the instrument and starting the measurement, we insert the sample only when prompted at 15 % of the scheduled measurement time, while holding the tube above the opening of the device until prompted. After the time has elapsed, the sample is released into the hole and removed from the device at 60 % of the measuring.

Fig. 12 Method of loading the sample into the FerroCheck 2000 device
Source: authors.

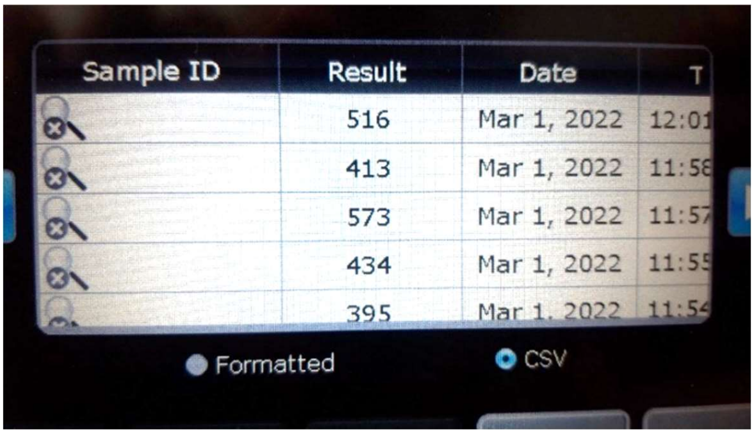

Fig. 13 Display with our measured values
Source: authors.

Following the completion of the measurement, we read the results of the amount of Ferroparticles from the device display, which we report in ppm (1 ppm = 0.0001 %). The following limitation was set for Ferroparticles for the assessment of motor oils:

Tab. 2 Limitations of content of Ferroparticles

Limitation	Amount of Ferro particles [ppm]
Occurrence of Ferroparticles	0-30
Increased amount of Ferroparticles	30-70
Risk amount of Ferroparticles	70-100
Intolerable amount of Ferroparticles	101 and more

Source: authors.

Tab. 3 Table of measured values

Parameter	1. Measurement	2. Measurement	3. Measurement	4. Measurement	5. Measurement	Average value
Ferroparticles (Fe,Co,Ni) [ppm]	395	434	573	413	516	466,2

Source: authors.

According to the average of the measured values of ferroparticles in Mogul Diesel DT SAE 20W-50 oil, it can be concluded that this used oil contains an intolerable amount of ferroparticles and is therefore not operational.

5 MEASUREMENT OF PROPERTIES OF MO-MOGUL DIESEL DT SAE 20W-50 ON SPECTROVISC Q3000

The SpectroVisc Q3000 Series Viscometer is a portable device used to measure the kinematic viscosity of oils and other lubricating fluids. To perform the measurement, a small sample of oil is placed on two metal surfaces, which, after closing them, form a tunnel and the sample flows to the bottom of the tunnel by microchannel. The sensor detects the flow rate across the cell and the device automatically calculates the kinematic viscosity value.

Before starting the measurement, it is necessary to thoroughly clean the test area of any residues of other oils or impurities that would adversely affect the measurement results.

The next step is to apply the oil sample itself to the test area of the instrument using a disposable or discharge pipette.

However, as with FerroCheck, it is necessary to mix the sample precisely here, after mixing and taking the sample into the pipette, we apply the tested oil to the pouring tunnel at a reasonable speed, taking care that the oil does not escape outside the channel.

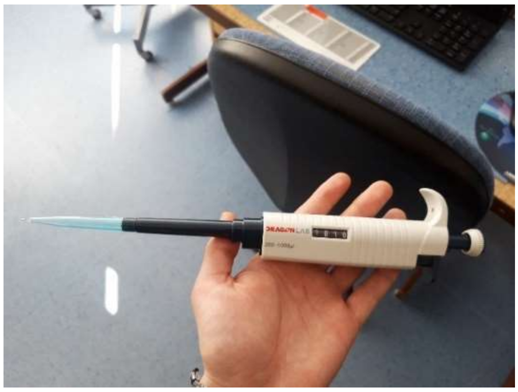

Fig. 14 Discharge pipette
Source: authors.

Fig. 15 Testing area of SpectroVisc Q3000
Source: authors.

5.1 Measurement

To measure the kinematic viscosity, we prepared a used sample of SAE 20W-50 oil, which we then compared with pre-measured values of the reference sample. Before starting the measurement, we thoroughly cleaned the test surface of the instrument according to the required procedure and took a suitable amount of oil sample into a disposable pipette, which we applied to the viscometer channel after the instrument prompt, after which we started measuring the kinematic viscosity on the device.

After displaying the measurement results on the screen of the device, we wrote down the given values and repeated the measurement twice more, we built a table from the recorded values as the next step.

Fig. 16 Application of oil sample
Source: authors.

Table 4 Measurements results of kinematic properties

Parameter	Unit	Reference sample SAE 20W-50	SAE 20W-50 test sample Measurement No.1	SAE 20W-50 test sample Measurement No.2	SAE 20W-50 test sample Measurement No.2	Arithmetic mean SAE 20W-50 test sample
Kinematic viscosity at 40 ° C	[cSt]	+20% 196,8 164 -20% 131,2	150 -8,54% -14	155 -5,5% -9	94,7 -42,26% -69,3	133,23 -28,77% -30,78
Kinematic viscosity 100 ° C	[cSt]	+20% 22,2 18,5 -20% 14,8	18,2 -1,63% -0,3	18,6 +0,54% +0,1	13,1 -29,19% -5,4	16,63 -10,11% -1,87
Viscosity index	-	130	-	-	-	-

Source: authors.

5.2 Measurement evaluation MO-Mogul Diesel DT SAE 20W-50

Reference sample No.R AFA

Kinematic viscosity at 40 ° C: COMPLIES [164 cSt. ± 20 % <131.2 cSt; 196.8 cSt>].

Kinematic viscosity at 100 ° C: COMPLIES [18.5 cSt. ± 20 % <14.8 cSt; 22.2 cSt>].

Used Sample MO-Mogul Diesel DT SAE 20W-50

Mileage since production 1,684 km

Mileage since MO exchange: 371 km

The oil was taken from the MAF body cleaner on 09.09.2020

Satisfactory book viscosity / 40 ° C: 133.23 [cSt], MO viscosity reduction is 30.78 [cSt] - Mo viscosity reduction by 28.77 [%]. The allowable tolerance is derived from a reference sample [164 cSt. ± 20 % <131.2 cSt; 196.8 cSt>]

COMPLIANT kinematic viscosity / 100 ° C: 18.5 [cSt],
MO viscosity reduction is 1.87 [cSt] - MO viscosity reduction is -10.11 % [%]. The allowable tolerance is derived from a reference sample [18.5 cSt. ± 20 % <14.8 cSt; 22.2 cSt>]

6 MEASUREMENT OF OIL PROPERTIES USING THE SPECTRO Q 1000 FLUIDSCAN

FluidScan measures the oil absorption spectrum in the mean IR range from 2.5 µm to 12 µm. To measure oil, diffraction is used, which uses an optical grating with a detector for better accuracy and durability. The patented switching top cell uses one drop of oil or a grease stain, does not take more than a minute to clean and does not require any chemicals or solvents. There is an integrated database of active information and pre-set alarm limits using the colour system for operation to ensure that relevant personnel can make decisions as soon as the measurement is made. FluidScan has algorithms for many of the world's most common types of lubricants. These algorithms provide calibration for most types of lubricants, so you do not need to physically measure a fluid sample to provide a basis for comparative analysis.

Fig. 17 Spectro Q 1000 Fluidscan
Source: author.

At the beginning of the measurement on this device using a clean pipette, place a drop of oil on the lower half of the glass of the test cells until it is properly blurred. Then we close the cell. To close the cell, fold the upper half of the cell until the lower half remains and release the magnets to close the magnets, then return the test cell to the drawer after this step and press the OK button to start measuring the sample. Based on the configured settings, the results will be displayed on the device screen when the measurement is completed.

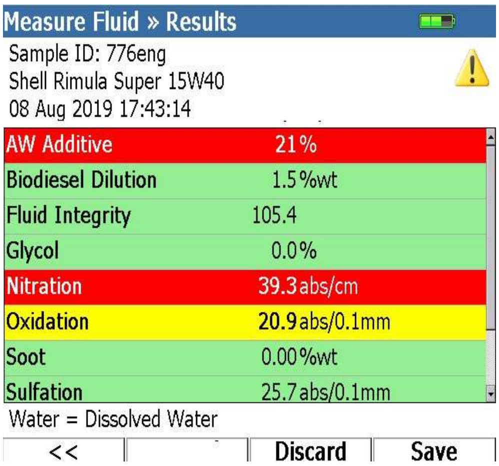

Fig. 18 Display of Spectro Q 1000 Fluidscan
Source: author.

6.1 Measurement

After following the procedures according to the device manual, the screen provided us with the measurement results, which we then entered the table.

- Alkalinity number (TBN) [mg KOH / g] / 7.4 / increase over R-AOS by 0.4 [mg KOH] not to allow engine oil operation when the TBN value decreases by more than 50% of the reference sample value. COMPLIES.
- Set [% w / t] / 0 / increase compared to R-AOS by 0 [% w / t] / maximum value is up to 2% w / t. COMPLIES.
- Oxidation [abs / 01] / 11.2 / increase compared to R-AOS by 0.8 [abs / 01] / do not allow MO operation when the value of antioxidant content decreases by more than 50% of the value of the reference sample. COMPLIES.
- Nitration-Nitridation [abs / cm] / xx / was not measured.
- Sulfation [abs / 01] / 18, an increase of 1.4 [abs / 01 / these processes in motor oil. They cause the decomposition of the components of the base oil and additives; the trigger is the presence of water in the MO - it is monitored in proportion to the presence of water
- Water content [ppm] / 902 / the reference sample was contaminated with water +563 ppm / monitored and the limit values of water content in motor oil are: 0.5% w / w / 5,000 ppm (risk factors are already concentrations 0.1 - 0 , 3% w / w / 1,000-3,000 ppm) / DOES NOT COMPLIES .
- Glycols [%] (0.0) same as R-AOS / The presence of glycols in the engine oil is not permitted. COMPLIES
- Addivation [%] / 108 / increase compared to R-AOS by 8 [%], (unknown additive added) / do not allow operation of engine oil when the value of total additive decreases by more than 50% / COMPLIES.

Table 5 Results of Measurement

Parameter	Unit	Reference sample SAE 20W-50	SAE 20W-50 test sample Measurement
TBN	[mg KOH/g]	7,0	7,4 (+0,4)
carbon black	[% w/t]	0,0	0
Oxidation	[abs/01]	11,2	12 (+0,8)
Nititation	[abs/cm]	-	-
Sulfation	[abs/01]	16,6	18 (+1,4)
Glykcols	[%]	0,0	0
Water content	[ppm]	339	902 (+563)
additive	[%]	100	108 (+8)

Source: authors.

7 OVERALL EVALUATION OF THE MEASURED SAMPLE MO-MOGUL DIESEL DT SAE 20W-50 USED SAMPLE THE MEASURED VALUES IN THE TRIBODIAGNOSTICS LABORATORY

The measured values in the tribodiagnostics laboratory showed that the tested oil is NOT SUITABLE the requirements, mainly due to the high content of ferroparticles and the amount of water. The total sample of MO-Mogul Diesel DT SAE 20W-50 must therefore be considered NOT SUITABLE for further operation.

8 CONCLUSION

In this work, I approached the basic properties, characteristics and parameters of motor oil Mogul Diesel DT SAE 20W-50 used in heavy machinery OS SR, such as Tank T-72M1. At the Department of Mechanical Engineering at the Academy of the Armed Forces, General: Štefánik in Liptovský Mikuláš, based on the knowledge gained so far in the field of tribodiagnostics, we subjected this oil to closer observation and research. A sample of this type of oil was examined in comparison with its reference sample. We subjected the oil to a closer examination of its kinematic properties, viscosity properties as well as its ferroparticle content. We have created tables for comparing the measured values in comparison with the reference sample for a simpler idea of the change in its properties as a result of its use. We drew partial conclusions from the measured results, which helped us to determine the ability of the used sample for further operation, while the results showed that the used oil Mogul Diesel DT SAE 20W-50 does not meet the standards and norms for its further use and replacement of this engine oil is necessary.

Acknowledgments:

This article was prepared on the basis of documents of the VV1 Project: Design and application of tribodiagnostic methodologies for operation and maintenance of ground equipment of the Armed Forces of the Slovak Republic in the years 2018 - 2020. The text of the report and pictorial documentation are originals.

References

[1] MARKO, M. Project VV1, Design and application of tribodiagnostic methodologies for operation and maintenance of ground equipment of the Armed Forces of the Slovak Republic in the years 2018 - 2020.

[2] Available at: https://eshop.paramo.cz/data/VyrobkovaDokumentace/bl10clp_mogul_diesel_dt20w50_z5.pdf

[3] Available at: https://slovakarmy.jex.cz/menu/t-72-m1

[4] Vojenská špecifikácia MSU, motorový olej SAE 30, 40, 50 (20W50), 10W30, 15W40, Edícia 11/2018.

Bc. Viktor **DOLINAJ**
Armed Forces Academy of General M. R. Štefánik
Department of Mechanical Engineering
Demänová 393
031 01 Liptovský Mikuláš
Slovak republic
E-mail: viktor.dolinaj@aos.sk

Dipl. Eng. Miroslav **MARKO**, PhD.
Armed Forces Academy of General M. R. Štefánik
Department of Mechanical Engineering
Demänová 393
031 01 Liptovský Mikuláš
Slovak republic
E-mail: mikro_makro@pobox.sk
miroslav.marko@aos.sk

Viktor DOLINAJ - was born on November 11, 1998 in Hnúšťa, Slovakia. He received your basic education in the years 2005 to 2014 at a school in Tisovec. In the years 2014 to 2018 he received a secondary education at SPŠ Strojnícka in Košice. In the years 2018 to 2021 he received a bachelor's degree from the Armed Forces Academy of General M. R. Štefánik in Liptovský Mikuláš.

Miroslav MARKO - was born on September 25, 1954 in Myjava, Slovakia. Between 1961 to 1970, he received his basic education in Stará Turá. Between 1970 to 1974, he received secondary education at the Grammar School in Nové Mesto nad Váhom. From 1974 to 1978 VVŠ PV, university education in the field of "Operation and repair of the tank and automotive technology". From 1991 to 1993 VŠPe, additional pedagogical study, Faculty of Education Nitra. In 1997 House of Technology ZSVTS, Slovak Society for Tribology and Tribotechnics, postgraduate one-year study in Tribotechnik, Bratislava. From 1999 to 2004 Military Academy, doctoral study - external, 91-06-9 Armament and ground forces technology, Liptovský Mikuláš in the field 20. May 2011 Tribotechnik II Certification - This is to certify that is qualfied for activities in technical diagnostics.

DOI: https://doi.org/10.52651/sam.a.2022.2.26-29

MEASUREMENT OF THE RESOLUTION OF THE MOUNTED PERISCOPE OF THE ARMOURED VEHICLE

Josef BAČA, Ivan PEMČÁK, Kateřina NOVÁČKOVÁ

Abstract: Resolution measurement of the night branch of the mounted device is investigated in this article. Measuring optical parameters of a mounted devices is a real problem that can improve the overall battle performance and effectivity of the armoured vehicle. The experimental verification is designed to be performed in field conditions with accessible equipment. To measure the resolution, it is needed to design corresponding test targets. To protect image intensifier from damage, it is necessary to use protection cover which attenuate incoming illumination. With decreased illumination the resolution of the imager also decreases, this hypothesis is demonstrated on experimental measurement.

Keywords: Night vision device; Night vision metrology; Optics, Fire-control system; Optical measurement

1 INTRODUCTION

Today, armoured vehicles are parts of every modern armed forces. They are equipped with a weapon turret which have a variety of reconnaissance optical devices that serve to obtain information about the target for fire-control system.

In the shadow of the weapon station optics, there are driver's periscopes. Driver's periscopes are used for driving the armoured vehicles when the driver needs to drive when covered. These periscopes consist of day periscope and night vision device with an image intensifier. (CHRZANOWSKI, 2015)

It is needed to give enough attention to the diagnostics of the driver periscopes because their failure can cause fatal damage to the vehicle and the crew. This is especially important in case of night branch.

Driver needs to have precise information about the road and its surroundings to be able to fulfil required tasks. Diagnostics of the periscopes is needed to be done on mounted devices because of the adjustment of the periscope itself. (Chrzanowski, 2022)

2 DETERMINATION OF BASICS PARAMETERS

For the beginning it is needed to set the basic parameters which are required for periscope to fulfil.

The day branch range when consists of an optical scope depends on the driver and his abilities and experience.

Night branch based on image intensifier range depends on image intensifies parameters and performance. In night conditions there is usually no backup way how to drive the vehicle when night branch fails.

Testing of image intensifier night devices during the day is complicated because it is needed to significantly decrease illumination of the device to prevent its damage. To solve this complication, it is possible to use a grey filter to decrease incoming illumination. (CHRZANOWSKI, 2015)

To be able to measure the parameters it is needed to set the measure conditions according to expected values.

For measured device, there are designed performance parameters from Tab. 1

Tab. 1 Device parameters

VIS branch	
Magnification	1x
Resolution	1' (standard human eye resolution)
Night branch	
Resolution	4' (standard temperature)
Range	recc straight road and terrain
3 mlx	120 m
50 mlx	400 m

Source: authors.

It is needed to transfer these values to corresponding resolution value.

From the designer information the maximal resolution is $x = 4' \approx 1.63$ mrad.

For reconnaissance it is needed to have 4 periods in the target width, then $x_r = 4x = 6.52$ mrad.

Then the minimal recognizable width of the road on the distance is

$$d = l \cdot x_r = [m], \tag{1}$$

where l is the range in km and x_r is angular width in mrad.

With decreasing irradiation of the imager, the resolution decreases.

3 RESOLUTION MEASUREMENT

To measure resolution on field conditions, there are used testing target images. These images have known properties which enables the measurement of the resolution of an imager. The most used images are Siemens star and USAF 1951 test. Tests are evaluated according to Johnson's criterion.

3.1 Siemens star

Siemens star consists of circle with black and white periods pattern that go from the centre and become wider on the edge of the circle. These periods have same angular size, and their count is the main parameter of the star. The resolution of the image is measured as a diameter of the unrecognizable grey middle circle in the picture. It can measure resolution in more directions at once, but it is needed to have captured image to evaluate the resolution from the image.

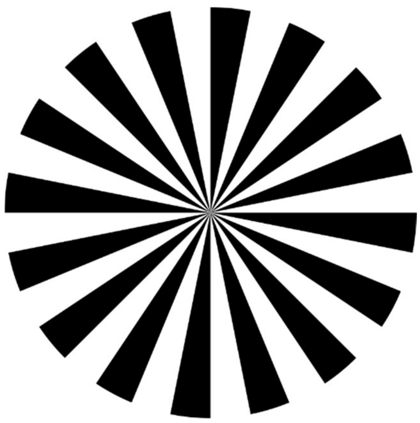

Fig. 2 Siemens star 16period
Source: [3].

Captured image with measured circle is shown in Fig. 2.

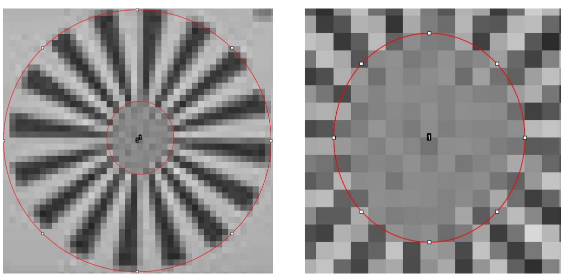

Fig. 2 Captured image of Siemens star
Source: authors.

Resolution of imager is then

$$h = \frac{\pi}{p} d_1, \quad (2)$$

where h is resolved period, p is number of periods of the star, d_1 is measured diameter of the unresolvable circle.

Resolution x in lp/mrad then

$$x = l/h \text{ [lp/mrad]} \quad (3).$$

where l is the distance to the target in m.

3.2 USAF test

The USAF 1951 resolution test (USAF test) according to MIL-STD-150A is a three-line test that is used to determine the resolution of a given imager. It consists of several groups of elements divided into 6 per group, arranged so that the even groups are in the left part of the test, except for the first element of the group, which is in the lower right corner, and the odd groups are in the right part of the test. Lower numbered groups are in the outer part and towards the center the groups get smaller.

Element dimensions are shown in Fig. 3.

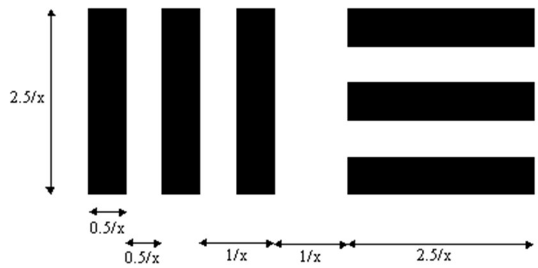

Fig. 3 Dimensions of an element in USAF 1951 test
Source: [3].

The whole test chart is shown in Fig. 4.

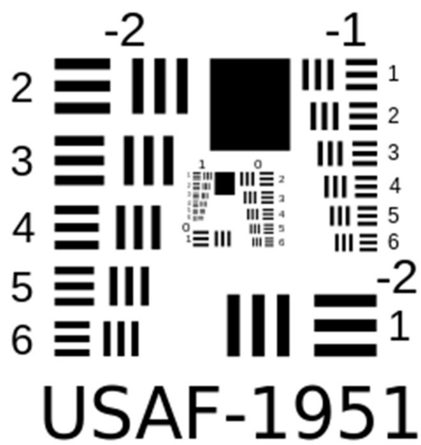

Fig. 4 USAF 1951 resolution test
Source: [4].

Resolution x of an imager is determined by the smallest resolved element in the chart.

$$x = 2^{\left(g + \frac{e-1}{6}\right)}\ [\mathrm{lp/mm}], \quad (4)$$

where g is group of the element and e is element number in the group.

This test can be evaluated directly using a naked eye without any need for capturing and computer evaluating. However, for objective evaluation and comparison with other tested imagers it is necessary to capture the image of testing chart.

3.2 Range calculation

When resolution is measured then range to certain target can be determined. There is wide-used criterion called Johnson's criterion which determines the range to the certain target according to width of the period in the required direction when the target is converted to black and white periods. (Sjaardema, Smith, & Birch, 2015)

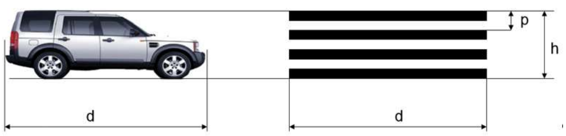

Fig. 5 Target conversion to period test
Source: [6].

According to number of the periods which can be resolved there are levels of the resolution of the target within certain probability. Usually there are 3 categories for 50 % probability of resolution. (Sjaardema, Smith, & Birch, 2015)

- 1 period for detection,
- 4 periods for reconnaissance,
- 8 periods for identification.

4 EXPERIMENTAL RESOLUTION MEASUREMENT

The goal of the experiment is to describe the effect of illumination decrease to resolution of the NV imager. (CHRZANOWSKI, 2015)

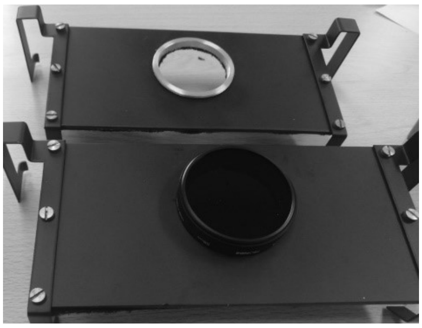

Fig. 6 Protective cover with off/on grey filters
Source: authors.

To demonstrate measuring of resolution change when illumination is decreased it was needed to make a protective cover to prevent damage of the device caused by daylight. The cover has in the optical axis of the objective a window which can be filled with grey filter of a known extinction ratio.

The cover protects the whole objective, the window has diameter of 58 mm and decreases the overall illumination of the objective 6 times without any filter. There are used grey filters that decreases the incoming illumination 8 or 64 times. When they are stacked, the combined decrease multiply. For the experiment is used total filter extinction from 2^{12} to 2^{21} (from 4096 to 2mil times). The illumination of the objective is 3.6 klx, the distance to the target is 4 m.

To control measurement is captured image from the day branch.

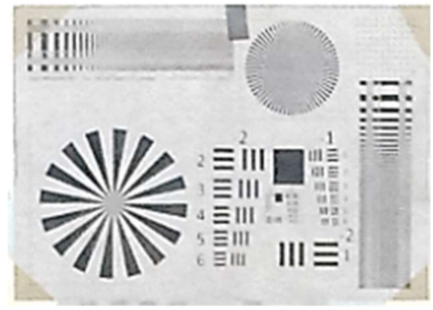

Fig. 7 Captured image from the day branch of the imager
Source: authors.

The Siemens star circle centre diameter is 18 mm which corresponds according to eq. (3) resolution of $x = 1.13$ lp/mrad. With USAF test the resolution was measured $x = 1.27$ lp/mrad.

For the measurement of the night branch USAF test was not usable, because even the biggest element was hardly resolvable. Only Siemens star resolution was used.

In the Tab. 2 there is resolution of the night branch with extinction filters applied.

Tab. 2 Measured values of Siemens star

Extinction	Ilumination	Siemens diameter	Resolution
ratio	mlx	mm	lp/mrad
4069	878,906	53	0,38
32768	109,863	76	0,27
262144	13,733	122	0,17
2097152	1,717	Non resolvable	0

Source: authors.

When the extinction coefficient decreased the illumination under 3 mlx, the image had become unresolvable

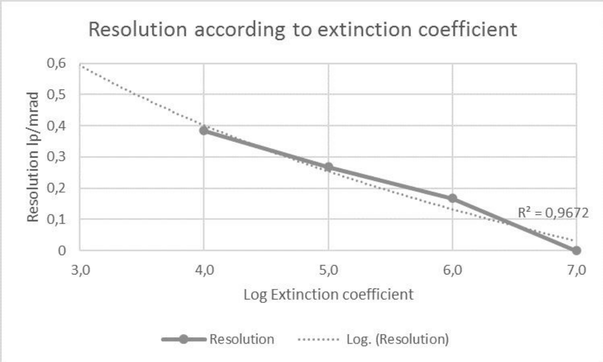

Fig. 8 Graph of the influence of the extinction ratio to the resolution of an imager
Source: author.

5 CONCLUSION

In this article, there was demonstrated the possibility of measuring the resolution of mounted night vision device in field conditions.

The ability to measure this property in real condition is necessary for analysis of performance of an armoured vehicle in real conditions. The research of these properties increases the combat capability and safety of the crew of the combat vehicle.

In this article it is presented the way of measuring the image intensifier device with variable extinction ratio of an incoming illumination. It is possible to simulate the threshold conditions of the device usage in field conditions.

There is demonstrated decreasing resolution with increasing extinction ratio. It was experimentally verified the lower threshold limit of needed incoming illumination is in the assumed interval.

In this article experimental measurement of resolution of night vision device was done. To develop this problematic further, it is needed to perform this measurement on widespread variety of devices.

References

[1] CHRZANOWSKI, K. Review of night vision metrology. In *Opto-Electronics Review,* vol. 23, no. 2, 2015, pp. 149-164. Available at: https://doi.org/10.1515/oere-2015-0024.

[2] CHRZANOWSKI, K. *Computerized station for testing night vision devices.* Inframet.com. [Online] 2022. [Citace: 20. 05 2022.] Available at: https://www.inframet.com/Data_sheets/NIMAX.pdf.

[3] ZEMAN, P. *Návrh pracoviště pro testování kvality OE přístrojů v podmínkách AČR.* [Diplomová práce] Brno: Univerzita Obrany v Brně, 2019.

[4] Arme forces supply support center. Military standard photographic lenses. Washington DC : Standardization division, Arme forces supply support center, 1959. MIL-STD-150A.

[5] SJAARDEMA, T. A., C. S. SMITH and G. C. BIRCH. *History and Evolution of the Johnson Criteria.* [online] United States: Available at: https://doi.org/10.2172/1222446.

[6] BALÁŽ, T. a Z. REHOŘ. *Dosahy OE přístrojů v reálných podmínkách.* [Online]. [Citace: 09. 05 2022] Available at: https://docplayer.cz/68745505-Dosahy-oe-pristroju-v-realnych-podminkach.html

Dipl. Eng. Josef **BAČA**
University of Defence
Kounicova 65
662 10 Brno
Czech Republic
E-mail: josef.baca@unob.cz

Dipl. Eng. Ivan **PEMČÁK**
University of Defence
Kounicova 65
662 10 Brno
Czech Republic
E-mail: ivan.pemcak@unob.cz

Dipl. Eng. Kateřina **NOVÁČKOVÁ**
University of Defence
Kounicova 65
662 10 Brno
Czech Republic
E-mail: katerina.novackova@unob.cz

Josef BAČA graduated in Weapons and ammunition engineering from University of Defense, Czech Republic in 2017. He serves in the military repair facility in Jaroměř, where he specializes in the repair of fire control systems. His field of research is fire control systems, target acquisition and optical system design.

Ivan PEMČÁK graduated in Weapons and ammunition engineering from University of Defense, Czech Republic in 2018. After two-year as an ordnance officer in a light infantry battalion of Czech armed forces, he returned to the University of Defense as Ph.D. candidate. His field of research is fire control systems, target hit probability and weapon design.

Kateřina NOVÁČKOVÁ graduated in Weapons and ammunition engineering from University of Defense, Czech Republic in 2022. She is now at the University of Defence as PhD candidate. Her field of research is optoelectronic devices, lasers and laser safety.

SCIENCE & MILITARY - WRITER´S GUIDELINES

1. Scientific articles submitted for publishing have to be original, topical and never been published before.

2. Articles have to be written in English language and in accordance with ethical standards. For more details, please visit the website of the Science & Military Journal (http://sm.aos.sk/index.php/en/for--authors-en/ethical-standards).

3. Length of the article should not exceed 6 pages in defined format. Microsoft Word text editor must be used for writing. Articles must be written using Times New Roman, single line spacing and follow the following form: Title -12 point bold capital letters aligned to the center. Full author´s (co-author´s) name – 10 point normal letters aligned to the center. Abstract – 9 point normal letters, extent 3-5 lines. Keywords – 9 point normal letters. The article text – 10 point normal letters. Contact - full author´s (co-author´s) name, affiliation, e-mail – 9 point normal letters at the end of the article. The article text will be written in 2 columns format with a 75 mm column width and 10 mm empty space separating the columns. The first line of each paragraph must be shifted 5 mm to the right.

4. Upper and lower margins must be set to 25 mm, left and right margins to 20 mm. Select mirror margins and set binding margins to 10 mm. The distance between the header/footer and the page margin must be 12,5 mm, while different odd and even pages must be selected.

5. Photographs for publication must be in black-white (not in color) of excelent quality with good contrast.

6. Equations in the text are also to be written using the equation editor. (Equation must be typed in Microsoft Equation, which is an integral part of Microsoft text editor.) They must be numbered. Numbers are to be enclosed in parentheses and aligned to the right margin of a column.

7. Figures, graphs and tables must be included in the text and numbered and must contain description. Figures must be identified as Fig. 1 followed gradually by the figure description. Graphs must be identified as Graph 1 followed by the graph description. Tables must be identified as Tab. 1, followed by the table description.

8. References must be fully and accurately documented (according to ISO 690). References should be quoted in the text in square brackets and listed in the order they have appear in the text.

9. The specimen article that can be found on the web-site: http://sm.aos.sk/index.php/en/for-authors-en can be used as an example of the correct format.

10. The editorial board will consider submitted articles in the next scheduled meeting. If it decides to include the article in the next issue it submits the manuscript to the editors for the peer review. The final version (before printing) will be sent to the author for the final revision. The authors are fully responsible for the level of language.

11. Contributions in A4 format edited according to the specimen article should be submitted in one hard copy and also in electronic form to the Editorial board.

12. The deadlines for the delivery of the articles in calendar year are: March 1 and September 1.

SCIENCE & MILITARY

No 2 | Volume 17 | 2022

Contents

ISSN 1336 – 8885 (print)
ISSN 2453 – 7632 (online)